Scale decomposition of molecular beam epitaxy

Z Moktadir

School of Electronics and Computer Science, Southampton University, UK

Abstract
In this work, a study of epitaxial growth was carried out by means of the wavelets formalism.
We showed the existence of a dynamic scaling form in a wavelet discriminated linear molecular
beam epitaxy (MBE) equation where diffusion and noise are the dominant effects. We
determined simple and exact scaling functions involving the scale of the wavelets when the
system size is set to infinity. Exponents were determined for both correlated and uncorrelated
noise. The wavelet methodology was applied to a computer model simulating linear epitaxial
growth; the results showed very good agreement with analytical formulation. We also
considered epitaxial growth with the additional Ehrlich–Schwoebel effect. We characterized the
coarsening of mounds formed on the surface during the nonlinear phase using the wavelet
power spectrum. The latter has an advantage over other methods, in the sense that one can track
the coarsening in both frequency (or scale) space and real space simultaneously. Wavelets
analysis also provides a quantitative tool for the characterization of the mounded surfaces
through its concise scale discrimination. We showed that the averaged wavelet power spectrum
(also called scalegram) over all the positions on the surface profile identified the existence of a
dominant scale a^*, which increases with time following a power law relation of the form
$a^* \sim t^n$, where $n \simeq 1/3$.

(Some figures in this article are in colour only in the electronic version)

1. Introduction

Over the last two decades, many aspects of molecular beam epitaxy (MBE) have been investigated theoretically within a phenomenological framework [1–4]. Phenomenological continuum models consider the surface of the growing film as a continuous variable of the position where overhangs are not allowed. They are credited with explaining many aspects of the surface morphology of growing films [5, 2]. The MBE process can be described as follows. Atoms are deposited on the film surface from the gas phase, where they undergo a thermally activated diffusion or desorption back to the gas phase. Once absorbed, atoms can combine to form a dimer, or attach to the steps of existing islands on the surface. A whole atomic layer is completed once all islands on the surface have coalesced. Smooth surfaces are obtained in a layer-by-layer growth mode in which a new layer starts to form only when the layer underneath is fully grown. However, experiments provide evidence that the layer-by-layer growth mode does not occur in many situations (see, for example, [6–8]). This ideal situation is suppressed by two dominant effects: shot

noise and instabilities that arise from the so-called Ehrlich–Schwoebel (ES) effect [9]. Shot noise originates from different mechanisms such as deposition, diffusion or nucleation. The ES effect is due to the asymmetry in attachment–detachment kinetics across an atomic step, where atoms have to overcome an energy barrier when descending the step. This triggers an ascending atomic current, which is responsible for a morphological instability. In this case, the amplitude of small perturbations on the flat surface will increase exponentially in time. This instability can be balanced by the introduction of a stabilizing mechanism such as a Mullins-like current arising from thermodynamic relaxation through surface diffusion [10] or from fluctuations in the nucleation process of newly forming islands [11, 12]. The ES effect and diffusion currents will induce the formation of a mound-like structure on the surface which coarsens as time progresses.

A phenomenological continuum model describing the surface growth incorporating the two conserving mechanisms mentioned above can be formulated in one dimension as:

$$\frac{\partial h}{\partial t} = -\nabla j_d - \nabla j_s + \eta(x, t) \qquad (1)$$

where h is the surface height, j_d is the ES destabilizing current, j_s is the Mullins stabilizing current and $\eta(x, t)$ is the noise function representing the stochastic character of the growth. This function is assumed to be a Gaussian white noise with zero mean, or a spatially correlated noise (long-range correlations), i.e.

$$\langle \eta(\mathbf{x}, t)\eta(\mathbf{x}', t') \rangle = 2F\delta(\mathbf{x} - \mathbf{x}')\delta(t - t')$$

$$\langle \eta(\mathbf{x}, t)\eta(\mathbf{x}', t') \rangle = 2F|\mathbf{x} - \mathbf{x}'|^{2\rho-1}\delta(t - t') \qquad (2)$$

where F is a constant and ρ $(0 < \rho < 1/2)$ is an exponent characterizing the decay of spatial correlations. The Fourier transform of the noise correlators above is given by:

$$\langle \eta(\mathbf{q}, t)\eta(\mathbf{q}', t') \rangle = 2F\delta(\mathbf{q} + \mathbf{q}')\delta(t - t')$$

$$\langle \eta(\mathbf{q}, t)\eta(\mathbf{q}', t') \rangle = 2D_\rho q^{-2\rho}\delta(\mathbf{q} + \mathbf{q}')\delta(t - t'). \qquad (3)$$

The prefactor D_ρ is given by:

$$D_\rho = \frac{F}{\pi}\int_0^\infty u^{2\rho-1}\cos(u)\,\mathrm{d}u = \frac{F2^{2\rho-1}\sqrt{\pi}\,\Gamma(\rho)}{\Gamma(1/2 - \rho)} \qquad (4)$$

where Γ is the gamma function.

A simple model for the currents j_d and j_s can be expressed as [11]:

$$j_d(m) = \nu\left(1 - \frac{m}{m_0}\right)$$

$$j_s(m) = -K\nabla^2(m) \qquad (5)$$

where $m = \frac{\partial h}{\partial x}$ is the surface slope. The parameters ν and K are positive constants related to microscopic processes of deposited atoms on the surface [13]. The parameter m_0 is the so-called *magic slope*. The form of the destabilizing current j_d predicts slope selection: the mound slopes will asymptotically reach a constant value m_0. Equation (1) has been investigated by mapping it to the phase ordering problem [14] or by mapping it to a one-dimensional system of interacting kinks [15]. The scenario predicted by (1) is the following. The competition between the ES effect and the surface diffusion will lead to a mound-like structured surface with a well-defined period. Later in time, the mounds will coarsen because of the nonlinearity of the current j_d. The period of the mounds $\lambda(t)$ scales with time as $\lambda(t) \sim t^n$, where $n = 1/3$ [15, 2].

The purpose of this paper is to characterize the MBE process described by (1) using the wavelets formalism. Two cases are considered here: linear stable growth where only surface diffusion and noise are taken into account, and growth incorporating the additional effect of an ES barrier. In the former case, the scaling functions and exponents are derived in wavelet space in the presence of both correlated and uncorrelated noise. In the latter case, the coarsening is discriminated through wavelet decomposition of the evolving surface profile and characterized by the wavelet power spectrum. The advantage of using wavelets is that one can track the coarsening process in real space and frequency space simultaneously. Wavelets analysis also provides a quantitative tool for the characterization of the mounded surfaces through its concise scale discrimination.

This paper is organized as follows. We first consider the linear stable MBE growth (section 2) by performing an analysis of growth in wavelet space. Section 3 is devoted to the nonlinear unstable MBE process. We close the manuscript with a conclusion.

2. The linear MBE

When diffusion is the dominant process in surface dynamics, all other destabilizing effects are neglected and (1) is reduced to a fourth-order linear form (for simplicity, we set $K = 1$):

$$\frac{\partial h}{\partial t} = -\nabla\mathbf{j}_s + \eta(x, t) = -\nabla^4 h(x) + \eta(x, t). \qquad (6)$$

In this section we will use the wavelet formalism in order to determine the properties of the linear MBE equation (6) through the scale discrimination of the growth process, that is, the determination of the scaling function and exponents as a function of the wavelet scale (see definition below) when the system size is infinite. The wavelet transform of a profile $h(x)$ is given by [16]:

$$T(a, x) = \frac{1}{\sqrt{a}}\int_{-\infty}^\infty h(y)\,\psi\left(\frac{y - x}{a}\right)\mathrm{d}y \qquad (7)$$

where a $(a > 0)$ is the scale parameter and ψ is the mother wavelet. The transform $T(a, x)$ is a scale-position decomposition which expands a function $h(x)$ in the wavelets basis, whose elements are constructed from a single mother function: the mother wavelet.

2.1. Dynamic scaling

In a previous work [20] we applied the wavelet formalism to the Edwards–Wilkinson equation. This investigation was concerned with dynamic scaling in terms of scale a but not the system size. We derived an exact and simple expression for the scaling function. The dependence of the surface width σ at a given wavelet scale was found to be a scaling law of the form $\sigma(a, t) \sim a$ for uncorrelated noise and $\sigma(a, t) \sim a^{\rho+1}$ for correlated noise. Here, we will apply the same formalism to (6). The lateral system size L is taken to be infinite and therefore the dependence on L is suppressed. Since each decomposition $T(a, x)$ does not result in a sine wave, it is possible to calculate its power spectrum. By a simple change of variable in (7), we compute the Fourier transform of each decomposition:

$$\hat{T}(a, q, t) = -\sqrt{a}\hat{h}(q, t)\int \psi(\xi)\,\mathrm{e}^{\mathrm{i}aq\xi}\,\mathrm{d}\xi$$

$$= -\sqrt{a}\hat{h}(q, t)\hat{\psi}(-aq) \qquad (8)$$

where $\hat{h}$ and $\hat{\psi}$ are the Fourier transforms of the height h and the mother wavelet ψ, respectively. The power spectrum at a scale a is then:

$$\Gamma(a, q, t) = \langle \hat{T}(a, q, t)\hat{T}(a, -q, t) \rangle = aP(q, t)|\hat{\psi}(-aq)|^2 \qquad (9)$$

The quantity $P(q, t)$ is the power spectrum of the surface height. Without loss of generality, one can use Hermitian
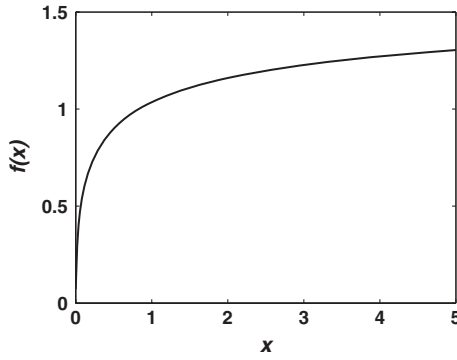
Figure 1. The scaling function $f(x)$.

Table 1. Values of the exponents in the two cases: the EW equation and the linear MBE equation in one dimension. Between the brackets are values of the exponents observed in the scaling with system size.

	α	z
EW	1(1/2)	2
MBE	2(3/2)	4

In one dimension, the scaling law dependence of the surface width at a scale a involves integer exponents in the two cases, the EW [17] and the linear MBE equations, unlike the scaling exponents observed in the dependence with the system size, which are fractional. Table 1 summarizes the value of exponents in both cases in one-dimensional space.

wavelets [17, 18] which are the successive derivatives of the Gaussian function $g_0(x) = \mathrm{e}^{-x^2/2}$. For the second-order Hermitian wavelet $\psi(x) = \mathrm{d}^2 g_0(x)/\mathrm{d}x^2 = -(1 - x^2)\mathrm{e}^{-x^2/2}$, the function $\hat{\psi}(q)$ is given by: $\hat{\psi}(q) = \sqrt{2\pi}q^2\mathrm{e}^{-q^2/2}$. By Fourier transforming (6), we obtain the solution for a flat initial condition of the surface profile $h(x)$:

$$\hat{h}(q, t) = \int_0^t \mathrm{e}^{q^4(\tau - t)}\hat{\eta}(q, \tau)\,\mathrm{d}\tau \qquad (10)$$

where $\hat{\eta}(q, t)$ is the Fourier transform of the noise η.

2.1.1. Uncorrelated noise. Using (10) and (3), the power spectrum of the surface profile is given by:

$$P(q) = 2F\frac{(1 - \mathrm{e}^{-2q^4 t})}{q^4}. \qquad (11)$$

We can now calculate the surface width at each scale. From (9) we get:

$$\sigma(a, t)^2 = \int_0^{q_{\max}} \Gamma(a, q, t)\,\mathrm{d}q$$
$$= a^5 F\pi \int_0^{q_{\max}} \left(1 - \mathrm{e}^{-2q^4 t}\right)\mathrm{e}^{-a^2 q^2}\,\mathrm{d}q. \qquad (12)$$

The upper cutoff $q_{\max}$ is of the order of the inverse lattice constant; we assume that the correlation length is larger than $1/q_{\max}$ and we set $q_{\max}$ to infinity in (12). Performing the integration, we arrive at:

$$\sigma(a, t)^2 = a^4 F\pi \left(2\sqrt{\pi} - \sqrt{\frac{a^4}{2t}}\mathrm{e}^{\frac{a^4}{16t}} K\left(1/4, \frac{a^4}{16t}\right)\right)$$
$$\propto a^4 f\left(\frac{t}{a^4}\right)^2 = a^4 f\left(\frac{t}{a^z}\right)^2 \qquad (13)$$

where the dynamic exponent $z = 4$, $f(x) = \sqrt{2\sqrt{\pi} - \frac{1}{\sqrt{2x}}\mathrm{e}^{\frac{1}{16x}} K(1/4, 1/(16x))}$ and $K(n, x)$ is the Bessel function of the second kind of order n. The saturation value of the width scales as $\sigma_{\mathrm{sat}} \propto a^\alpha$, with $\alpha = 2$. The scaling function $f(x)$ is not defined at $x = 0$, but has the asymptotic limit $f(x) \approx x^{1/2}$ for $x \ll 1$ (this is easily shown by performing a series development to the second order of $f(x)$) and $f(x) \approx \sqrt{2}\pi^{1/4}$ for $x \gg 1$. This function is displayed in figure 1.

2.1.2. Correlated noise. Similar to the above calculations, we will determine a different set of exponents by computing the surface width corresponding to each wavelet scale a taking the substrate size to be infinite, in the case of spatially correlated noise. We have the power spectrum of the surface profile h:

$$P_\rho(q) = 2D_\rho q^{-2\rho}\frac{(1 - \mathrm{e}^{-2q^4 t})}{q^4}. \qquad (14)$$

Using (9), we get, for the surface width at the scale a:

$$\sigma_\rho(a, t)^2 = \int_0^\infty \Gamma(a, q, t)\,\mathrm{d}q$$
$$= 2a^5 D_\rho\pi \int_0^\infty q^{-2\rho}\left(1 - \mathrm{e}^{-2q^4 t}\right)\mathrm{e}^{-a^2 q^2}\,\mathrm{d}q. \qquad (15)$$

In this integration we have taken the upper cutoff to be infinite. By a simple change of variable we have:

$$\sigma_\rho(a, t)^2 = \pi D_\rho a^{4+2\rho} \int_0^\infty \xi^{-\rho-1/2}(1 - \mathrm{e}^{-2\xi^2 t/a^4})\mathrm{e}^{-\xi}\,\mathrm{d}\xi$$
$$\propto a^{4+2\rho} f_\rho\left(\frac{t}{a^4}\right)^2 = a^{4+2\rho} f_\rho\left(\frac{t}{a^z}\right)^2. \qquad (16)$$

Here, $f_\rho(x)^2 = \int_0^\infty \xi^{-\rho-1/2}(1 - \mathrm{e}^{-2\xi^2 x})\mathrm{e}^{-\xi}\,\mathrm{d}\xi$ is a scaling function which has the limit $f_\rho(x) \approx \sqrt{x}$ for $x \ll 1$ and $f_\rho(x) \approx \sqrt{\Gamma(1/2 - \rho)}$, for $x \gg 1$, where Γ is the gamma function. The result for the uncorrelated case is retrieved for $\rho = 0$. Thus, for correlated noise, the roughness exponent is $\alpha(\rho) = 2 + \rho$ while $z = 4$, independent of ρ. For the EW growth model, the roughness exponent was found to be $\alpha_{\mathrm{EW}} = 1 + \rho$ [20].

2.2. Application to a computer model of the linear MBE

In this section we will apply the wavelets analysis to a computer model that simulates linear molecular beam epitaxy in the case of uncorrelated noise. This model was developed in [21] to simulate linear growth where diffusion is the dominant process. In this model, atoms are randomly deposited on a linear substrate and undergo diffusion to neighboring sites in order to maximize their curvature κ. If the height at a site i is $h(i)$, then the deposited atom at this site will move to a site j with the maximum value of $\kappa = h_{j+1} - 2h_j + h_{j-1}$. The diffusion length l is such that $i - l \leqslant j \leqslant i + l$.
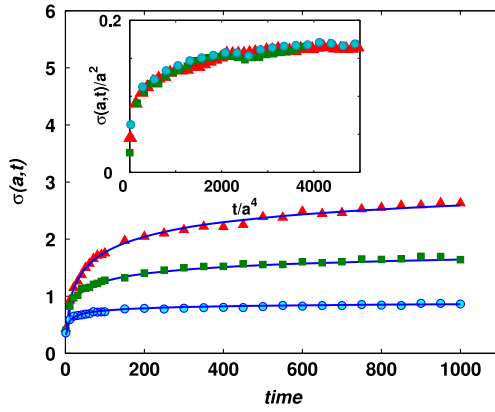
Figure 2. Computer simulation results showing the evolution of the surface width for three different scales: $a = 2$ (○), $a = 3$ (□) and $a = 4$ (△). Full lines are the fits to the analytical expression (13). The inset shows the data collapse to a single curve, confirming dynamic scaling form (13).

Figure 3. Color map plots showing the time evolution of the wavelet's power spectrum of the evolving profile for three different times: $t = 100$, 500 and 1000. The early stage ($t = 100$) shows the power concentration in a small band of scales surrounding the dominant scale as a result of linear instability. As time advances, the formed pattern moves towards larger scales as a result of the coarsening of mounds. The color scale is in arbitrary units.

Simulation is carried out for $l = 2$ and a substrate size $L = 10^6$ sites. Periodic boundary conditions were imposed. In figure 2 we show the plot of the surface width calculated at wavelet scales $a = 2$, 3 and 4 by performing the wavelet transform of the simulated profile and by using the expression $\sigma(a, t) = \langle (T(a, i) - \overline{T}(a))^2 \rangle_i$, where $\overline{T}(a)$ is the spatial average of $T(a, i)$, $i = 1, \ldots, L$. As can be seen, there is excellent agreement between the simulated value of $\sigma(a, t)$ and the scaling form (13). The inset of figure 2 shows good data collapse, confirming the scaling form (13).

3. Growth with Ehrlich–Schwoebel barrier

The current form j_m in (5) represents a continuous uphill current leading to a slope selection, i.e the mound's slope converges to a constant value m_0. This current is countered by the diffusion current j_d, preventing an indefinite increase in the mound's height. A simple linear stability analysis of (1) shows that this growth process is unstable against small perturbations with wavenumbers smaller than a critical value $q_c = \sqrt{\nu/K}$. This implies that the initial growth stage is characterized by the formation of mounds on the surface with the typical size $\lambda = 2\pi\sqrt{2}/q_c$. After this initial phase, nonlinearities become relevant, triggering the coarsening of mounds. The scaling hypothesis implies that the coarsening behavior is statistically self-similar, i.e. surface mounds are similar in time domain up to a scaling by the average mound size λ. Under the scaling hypothesis, structure functions such as the height–height correlation function can be written as $C(r) = \sigma(t)^2 \theta(r/\lambda(t))$, where σ is the surface width and θ is a scaling function. The evolution of λ and σ is expressed as:

$$\lambda \sim t^n \qquad \sigma \sim t^\beta. \qquad (17)$$

The current form given by (5) leads to slope selection, and the value of the scaling exponent is $n = \frac{1}{3}$ [4].

We will show in the following that the coarsening process can be well characterized by the wavelets formalism. The advantage of this formalism is that one can track the
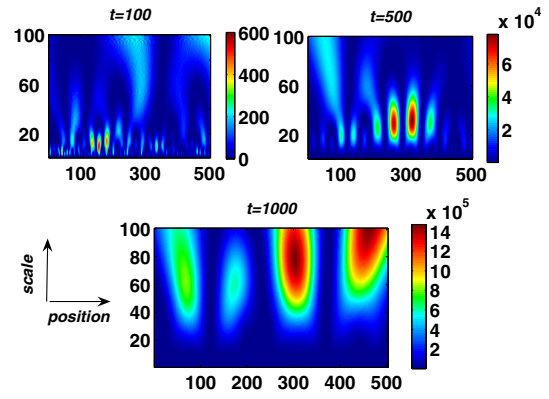
coarsening in both scale (or frequency) and the spatial position simultaneously. In addition, we can quantify the coarsening process by computing the evolution of a quantity called the *scalegram* [17], which is the counterpart of the power spectrum in Fourier analysis. We first start by solving (1) numerically using the third-order Adams–Bashforth scheme [19], where the time step is chosen to be small enough to ensure stability and convergence (the spatial resolution was set to $\Delta x = 1$). The current functions (5) were used and the periodic boundary conditions were imposed. The wavelet transform of the generated profiles is then computed at different times. The wavelet's power spectrum is defined as the squared magnitude of the wavelet transform, which is the analog of the power spectrum in Fourier analysis. Figure 3 displays the time evolution of the wavelet power spectrum at $t = 100$, 500 and 1000 for $\nu/K = 2$ and $L = 500$; the result is averaged over 100 independent runs. For simplicity, the Hermitian wavelet of order one is used in these calculations. We can clearly notice the pattern formed at the early stage of growth where the power is concentrated around the dominant scale as a result of the linear instability. As time advances, the pattern that is formed moves towards larger scales, indicating the coarsening process.

In general, the mound's coarsening is characterized by the determination of the lateral correlation length or by determining the wavenumber corresponding to the maximum of the Fourier power spectrum. The latter is related to the mound size λ via the relation $q_{max} = 2\pi/\lambda$. One can efficiently characterize the coarsening process by performing the calculation of the scalegram [17]. The scalegram is the spatial average of the wavelet power spectrum, i.e.

$$S(a, t) = \langle |T(a, x, t)|^2 \rangle_x. \qquad (18)$$

One of the main advantages of the scalegram over the Fourier power spectrum is the fact that only few realizations are required to obtain an accurate scalegram. We can show that this quantity defines a dominant scale at which it reaches its maximum value. We can obtain an analytical form of S as a
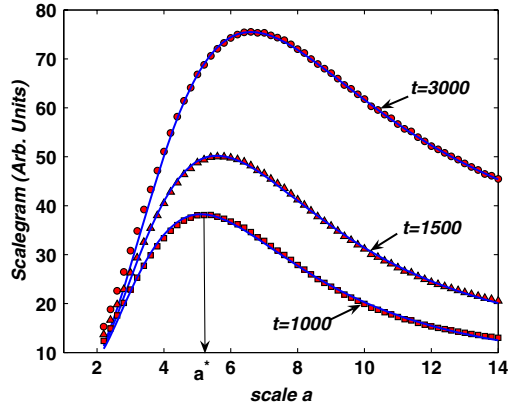
Figure 4. Plots of the scalegram obtained by numerical simulation at three different times: $t = 1000$ (squares), 1500 (triangles) and 3000 (circles). Continuous lines are fits to the analytical form (21).
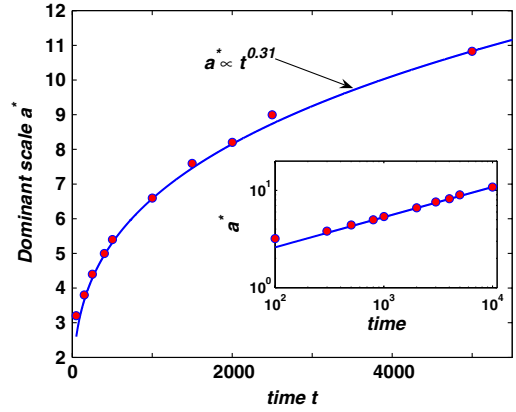

Figure 5. The evolution of the dominant scale (corresponding to the maximum of the scalegram) obtained from numerical simulations, showing a power law scaling with an exponent $n \simeq 1/3$. The inset shows the same result in a log–log plot.

function of the scale a and the mound size $\lambda = \lambda(t)$. Using the wavelet definition (7), we have:

$$S(a) = a^2 \iint \langle h(x + \xi a)h(x + \zeta a)\rangle_x \psi(\xi)\psi(\zeta)\,d\xi\,d\zeta$$
$$= a^2 \int \int C(\xi, \zeta, a)\psi(\xi)\psi(\zeta)\,d\xi\,d\zeta. \tag{19}$$

The kernel $C(\xi, \zeta, a) \equiv \langle h(x+\xi a)h(x+\zeta a)\rangle$ is the two-point correlation function which depends only on the difference $|(\xi - \zeta)a|$ for the present process, i.e. $C(\xi, \zeta, a) = C(|(\xi - \zeta)a|)$. We will choose the following form for $C(r)$ [22]:

$$C(r) = \sigma^2 e^{-\frac{r^2}{l^2}} \cos\left(\frac{2\pi r}{\lambda}\right) \tag{20}$$

where σ is the surface width and l is a parameter characterizing the decay of the correlations. The lateral correlation length is defined as $C(r) = \sigma^2/e$ and it is a function of both l and λ. To obtain a simple analytical form of S, we use the Hermitian wavelet of order one ($\psi(x) = -xe^{-x^2/2}$). Integrating (19) in $(-\infty, +\infty)$ and using (20), we have:

$$S(a) = f(a, \lambda, l)e^{-\frac{4\pi^2 a^2 l^2}{(4a^2+l^2)\lambda^2}} \tag{21}$$

where

$$f(a, \lambda, l) = \frac{4\pi a^4 \sigma^2 l(2\pi^2 l^4 + l^2\lambda^2 + 4a^2\lambda^2)}{\lambda^2(4a^2 + l^2)^{5/2}}. \tag{22}$$

We determined the scalegram from numerical simulations of (1) by computing the wavelet transform of the obtained profile and using the definition (18). Figure 4 shows the results at three different times: $t = 1000$, 1500 and 3000. The Hermitian wavelet of order one was used with a system size of $L = 500$. The ratio ν/K was set to 1.5, and the result was averaged over 100 independent runs. As can be seen, the agreement between numerical solution and the analytical form of the scalegram is extremely good. Equation (21) predicts the existence of a dominant scale a^*, which maximizes S, proportional to λ. Thus, the dominant scale evolves following the same power law followed by λ, i.e. (17).

This result is not surprising, since the continuous wavelet transform gives information as to the extent to which the frequency content of the analyzed profile, in the neighborhood of an arbitrary position x, is close to the frequency content of the wavelet at a given scale. To check the validity of the above, we numerically computed the value of the dominant scale as a function of time. This is shown in figure 5. The power law nonlinear regression fit is also shown with an exponent $n = 0.31 \pm 0.01$, a value consistent with the coarsening exponent $n = 1/3$. A log–log plot of the result is also displayed at the inset of figure 5, confirming the power law scaling.

4. Conclusion

In conclusion, we investigated epitaxial growth using the wavelets formalism. Two cases were considered: the linear case where only atomic diffusion is the dominant process, and the case where both atomic diffusion and the Ehrlich–Schwoebel barrier are the dominant processes. In the former case, the linear equation is decomposed using a wavelet filter, allowing the discrimination of growth dynamics at each scale. We determined the scaling functions of the width corresponding to each wavelet decomposition of the surface profile in two cases: growth with uncorrelated noise and growth with correlated noise. Analytical results were compared to a computer model simulating the linear growth in the case of uncorrelated noise. Good agreement was found between theory and computer simulation.

Growth incorporating the ES effect alongside atomic diffusion is characterized by numerically computing the wavelet power spectrum. The coarsening process is quantified by the so-called scalegram, which revealed a time-dependent dominant scale where the scalegram reaches its maximum. The dominant scale is proportional to the mound size, i.e. following a power law with an exponent $n \simeq 1/3$. An analytical form of the scalegram is determined as a function of the scale and the mound size. This analytical form was compared to numerical results, showing good agreement between the two.

The wavelet formalism has an advantage over Fourier methods in the way that one can track the coarsening in the location (direct space) and at different scales at the same time. It also provides a quantitative tool for the characterization of mounded surfaces.

References

[1] Krug J 1999 *Physica* A **263** 170
[2] Krug J 2002 *Physica* A **313** 47
[3] Politi P, Grenet G, Marty A, Ponchet A and Villain J 2000 *Phys. Rep.* **324** 271
[4] Torcini A and Politi P 2002 *Eur. Phys. J.* B **25** 519
[5] Siegert M and Plischke M 1994 *Phys. Rev. Lett.* **73** 517
[6] Kalf M, Smilauer P, Comsa G and Michely T 1999 *Surf. Sci.* **426** L447
[7] Van Nostrand J E, Chey S J, Hasan M-A, Cahill D G and Greene J E 1995 *Phys. Rev. Lett.* **74** 1127
[8] Evansa J W, Thiel P A and Bartelt M C 2006 *Surf. Sci. Rep.* **61** 1
[9] Ehrlich G and Hudda F 1966 *J. Chem. Phys.* **44** 1039
[10] Mullins W W 1957 *J. Appl. Phys.* **28** 333
[11] Politi P and Villain J 1996 *Phys. Rev.* B **54** 5114
[12] Politi P and Villain J 1997 *Surface Diffusion: Atomistic and Collective Processes* ed M C Tringides (New York: Plenum) p 177
[13] Pimpinelli A and Villain J 1998 *Physics of Crystal Growth* (Cambridge: Cambridge University press)
[14] Bray A J 1994 *Adv. Phys.* **43** 357
[15] Politi P 1998 *Phys. Rev.* E **58** 281
[16] Addison P S 2002 *The Illustrated Wavelet Transform Handbook* (Bristol: Institute of Physics Publishing)
[17] Moktadir Z 2004 *Phys. Rev.* E **70** 011602
[18] Lawalle J 1997 *Phys. Rev.* E **55** 1590
[19] Hoffman Joe D 2001 *Numerical Methods for Engineers and Scientists* (Boca Raton, FL: CRC press)
[20] Moktadir Z 2005 *Phys. Rev.* E **72** 011608
[21] Krug J 1994 *Phys. Rev. Lett.* **72** 2907
[22] Zhao Y-P, Yang H-N, Wang G-C and Lu T-M 1998 *Phys. Rev.* B **57** 1922